

## Direct experimental test of scalar confinement

Theodore J. Allen

*Department of Physics, Hobart & William Smith Colleges,  
Geneva, New York 14456, USA*

M.G. Olsson and Yu Yuan

*Department of Physics, University of Wisconsin,  
1150 University Avenue, Madison, Wisconsin 53706, USA*

Jeffrey R. Schmidt

*Department of Physics, University of Wisconsin-Parkside,  
900 Wood Road, Kenosha, Wisconsin 53141, USA*

Siniša Veseli

*Fermi National Accelerator Laboratory, P.O. Box 500, Batavia, Illinois 60510, USA*

The concept of Lorentz scalar quark confinement has a long history and is still widely used despite its well-known theoretical faults. We point out here that the predictions of scalar confinement also conflict directly with experiment. We investigate the dependence of heavy-light meson mass differences on the mass of the light quark. In particular, we examine the strange and non-strange  $D$  mesons. We find that the predictions of scalar confinement are in considerable conflict with measured values.

### I. A LITTLE HISTORY

Within a year of the discovery of charmonium in 1974, a picture emerged of two massive quarks moving in the QCD motivated static potential [1],

$$V(r) = -\frac{k}{r} + ar. \quad (1)$$

Here the color Coulomb constant  $k$  is given by  $k = 4\alpha_s/3$  in lowest order perturbation theory and  $a$  is the confinement constant, or asymptotic confining force. The non-relativistic Schrödinger equation accounted in a natural way for the spin averaged  $c\bar{c}$  and  $b\bar{b}$  spectra and decay rates [2]. It was soon realized that in order to understand the spin dependence of the heavy onia states one must further specify the Lorentz transformation properties of the interaction. Henriques, Kellett, and Moorhouse [3] proposed that the short range Coulombic part was a Lorentz vector and the long range confining part a Lorentz scalar. The reasoning by the above group and others [2, 4] was that in order to account for observations, the spin-orbit interaction must be suppressed by a partial cancelation between the short-range and long-range contributions.

This picture flourished unchallenged for fifteen years despite the lack of success in formally relating scalar confinement to QCD. Around 1990, the work of the Milan group [5] clarified this question dramatically. Using the low velocity Wilson loop formalism pioneered by Eichten and Feinberg [6], and later by Gromes [7], they found both the spin-dependent and spin-independent relativistic corrections in heavy onia. Their astounding result was that the long-range spin-independent QCD corrections differed from those of scalar confinement, though

the long-range spin-orbit corrections were the same pure Thomas ones given by scalar confinement. These results were subsequently verified by lattice simulations of QCD [8].

Because the spin-independent relativistic corrections to scalar confinement are incorrect, the scalar confinement scenario should logically be discarded. Indeed, the whole concept of potential confinement is in error. Fortunately, there is an alternative physical picture that can be employed. Back in 1982, Buchmüller [9] pointed out that a color electric flux tube should automatically yield the desired pure Thomas spin-orbit interaction because there is no color magnetic field in the quark rest frame. In 1992, it was shown that the spin-independent relativistic corrections [10] to the flux tube model exactly matched the QCD predictions [5]. Recently, we have constructed a consistent classical action for spinning quarks connected by a QCD string (flux tube) [11]. Hence there exists a simple physical picture that is consistent in many ways with QCD and is not a simple potential model.

Although inconsistent with QCD, scalar confinement models remain popular, probably because of their relative ease of solution. In this paper we point out an instance where the predictions of spin-independent scalar confinement disagree directly with experiment. We consider here the dependence of heavy-light (HL) meson masses on the light quark mass. We discuss a general HL potential model wave equation in Sec. II and exhibit a simple analytic perturbative solution for scalar confinement. We demonstrate the high accuracy of our numerical solutions by comparing them to the analytic ones. In Sec. III we collect and discuss the experimental data which we will compare to our predictions. In particular, we will establish that spin splittings do not depend on the mass of the light quark. Comparison of three confinement scenarios

to data is given in Sec. IV, where we give theoretical values obtained by exact numerical solution of the spinless Salpeter equation for both scalar and time component vector (TCV) confinement as well as flux tube confinement. Our conclusions in Sec. V are that scalar confinement predictions of the light quark mass dependence are not good and can be clearly seen in the difference of  $S$ -wave and  $P$ -wave meson states. We note further that electric (TCV) confinement also does not account for this difference but that the flux tube model exhibits remarkable agreement with experimental data.

## II. SCALAR CONFINEMENT EQUATION: A PERTURBATIVE SOLUTION AND AN EXACT NUMERICAL SOLUTION

### A. The heavy-light potential model

We consider a spinless quark of mass  $m$  that moves in a potential field. We assume that this field consists of central Lorentz scalar and time component vector fields,  $S(r)$  and  $V(r)$  respectively. The expected Lagrangian for this system is

$$L = -m(r)\sqrt{1 - \mathbf{v}^2} - V(r), \quad (2)$$

$$m(r) = m + S(r). \quad (3)$$

The momentum and Hamiltonian are then

$$\mathbf{p} = m(r)\gamma\mathbf{v}, \quad (4)$$

$$H = \mathbf{v} \cdot \mathbf{p} - L, \quad (5)$$

where  $\gamma = 1/\sqrt{1 - \mathbf{v}^2}$ .

By squaring  $\mathbf{p}$ , we see that

$$m(r)\gamma = \sqrt{\mathbf{p}^2 + m(r)^2}. \quad (6)$$

Substitution into the Hamiltonian (5) then yields

$$H = \sqrt{\mathbf{p}^2 + (m + S(r))^2} + V(r). \quad (7)$$

For a state of definite angular momentum  $\ell$  the momentum square can be written

$$\mathbf{p}^2 = p_r^2 + \frac{\ell(\ell + 1)}{r^2}. \quad (8)$$

With the usual replacement  $p_r^2 \rightarrow -\frac{1}{r}\frac{d^2}{dr^2}r$ , we obtain a wave equation that can always be solved numerically [12].

### B. A perturbative estimate of the light quark mass dependence

We next consider a simple model with scalar confinement,  $S(r) = a|\mathbf{r}| = ar$  and a time component vector

short range interaction,  $V(\mathbf{r}) = -\frac{k}{|\mathbf{r}|} = -\frac{k}{r}$ . From the general Hamiltonian (7), we find

$$H = \sqrt{\mathbf{p}^2 + (m + ar)^2} - \frac{k}{r}. \quad (9)$$

We wish to treat the short range parameter  $k$  and the light quark mass  $m$  as small perturbations. In the case where both  $k$  and  $m$  vanish, the zeroth order Hamiltonian is

$$H_0 = \sqrt{\mathbf{p}^2 + (ar)^2}. \quad (10)$$

The Hamiltonian  $H_0$  has the same eigenstates as its square which, with the replacements of Eq. (8) and  $p_r^2 \rightarrow -\frac{1}{r}\frac{d^2}{dr^2}r$ , leads to the harmonic oscillator equation,

$$\frac{d^2u_0}{dr^2} + \left(E_0^2 - \frac{\ell(\ell + 1)}{r^2} - a^2r^2\right)u_0 = 0, \quad (11)$$

where in the limit of small  $r$ ,  $u_0 \rightarrow r^{\ell+1}$  and  $u_0$  is normalized to

$$\int_0^\infty dr |u_0|^2 = 1. \quad (12)$$

The solution for the wave function and eigenvalue is standard;

$$u_0(r) = \mathcal{N}_{n,\ell} r^{\ell+1} e^{-\frac{1}{2}ar^2} L_{n-1}^{\ell+\frac{1}{2}}(ar^2), \quad (13)$$

$$\mathcal{N}_{n,\ell}^2 = \frac{2a^{\ell+\frac{3}{2}}(n-1)!}{\Gamma(\ell+n+\frac{1}{2})}, \quad (14)$$

$$E_0^2 = 2a \left(\ell + 2n - \frac{1}{2}\right). \quad (15)$$

Here  $L_{n-1}^{\ell+\frac{1}{2}}(ar^2)$  is the usual Laguerre polynomial,  $n$  is a positive integer starting with 1, and  $\ell$  is a non-negative integer starting with zero.

We now determine the effect of turning on  $k$  and  $m$  using the Feynman-Hellmann theorem [13],

$$\partial E / \partial \lambda = \langle \partial H / \partial \lambda \rangle, \quad (16)$$

where  $\lambda$  is any parameter of the Hamiltonian. Taking the expectation values using the  $k = m = 0$  wavefunctions (13) will yield an expansion in these parameters. To leading order we have

$$E = E_0 - k \langle r^{-1} \rangle + \frac{ma}{E_0} \langle r \rangle + \dots \quad (17)$$

The expectation values are worked out in general in the Appendix. Here we only consider the  $m$  and  $k$  dependence of the  $1S$  and  $1P$  states (i.e.,  $n = 1$  and  $\ell = 0$  and 1). The results are,

$$\langle r^{-1} \rangle_{1S} = 2\sqrt{\frac{a}{\pi}}, \quad (18)$$

$$\langle r^{-1} \rangle_{1P} = \frac{4}{3} \sqrt{\frac{a}{\pi}}, \quad (19)$$

$$\langle r \rangle_{1S} = \frac{2}{\sqrt{\pi a}}, \quad (20)$$

$$\langle r \rangle_{1P} = \frac{8}{3\sqrt{\pi a}}. \quad (21)$$

Using Eq. (17), we obtain the  $m$  dependence near  $k = m = 0$  ( $m$  slope) for the energies,

$$\frac{dE_{1S}}{dm} = \frac{2}{\sqrt{3\pi}} = 0.6515, \quad (22)$$

$$\frac{d(E_{1P} - E_{1S})}{dm} = \frac{2}{\sqrt{3\pi}} \left( \frac{4}{\sqrt{15}} - 1 \right) = 0.0214. \quad (23)$$

Again using Eq. (17) we obtain the  $k$  dependence near  $k = m = 0$  ( $k$  slope) for the energies,

$$\frac{1}{\sqrt{a}} \frac{dE_{1S}}{dk} = -2\sqrt{\frac{1}{\pi}} = -1.128, \quad (24)$$

$$\frac{1}{\sqrt{a}} \frac{d(E_{1P} - E_{1S})}{dk} = \frac{2}{3}\sqrt{\frac{1}{\pi}} = 0.376. \quad (25)$$

### C. Consistency of the exact numerical solution and the analytic perturbative solution

Before we proceed to a detailed comparison of the predictions of scalar confinement with the experimental data, we pause to verify the accuracy of our numerical method. In particular, we compare our analytic values for the slopes at  $m = k = 0$  in Eqs. (22) to (25) with our numerical method. This step is important because a general analytic solution of the spinless Salpeter equation is not known. Only for the remarkable case of a massless particle and linear scalar confinement, which is equivalent to the non-relativistic harmonic oscillator, can one obtain an analytic solution. In the general case, one must rely on exact numerical solutions. Some time ago, we introduced [12] a variational method, the Galerkin method, into particle physics to solve the spinless Salpeter equation with a time component vector interaction. This very robust method is applicable to a wide range of differential and integral equations. The method has been sharpened over the years by many authors [14]. One can cope with eigenvalue equations for operators that are complicated functions of both momenta and coordinates, such as the scalar confinement Hamiltonian (9), by using basis functions that can be Fourier transformed. We have performed a careful numerical solution of the eigenvalue equation for the Hamiltonian (9), for small  $k$  and  $m$ , and found the  $m$  and  $k$  slopes. The results are in excellent agreement with the values obtained by analytic calculation in Eqs. (22) through (25).

## III. EXPERIMENTAL DATA

### A. Spin splitting is independent of light quark mass

We first use experimental data to demonstrate, rather conclusively, that spin splittings within a given orbital angular momentum multiplet do not depend on the light quark mass. In particular, we consider several heavy-light meson spin multiplets in which both the strange and non-strange members have been observed [15]. First we examine the  $D$  and  $D_s$  type mesons with  $\ell = 0$  ( $S$ -waves). The hyperfine splittings for  $D_s$  and  $D$  mesons are

$$\begin{aligned} D_s^* - D_s &= 143.8 \pm 0.4 \text{ MeV}, \\ D_{\pm}^* - D_{\pm} &= 140.64 \pm 0.10 \text{ MeV}, \\ D_0^* - D_0 &= 142.12 \pm 0.07 \text{ MeV}. \end{aligned} \quad (26)$$

The corresponding  $S$ -wave hyperfine splittings for  $B$  type states are

$$\begin{aligned} B_s^* - B_s &= 47.0 \pm 2.6 \text{ MeV}, \\ B^* - B &= 45.78 \pm 0.35 \text{ MeV}. \end{aligned} \quad (27)$$

It is clear that the substitution of a strange quark for a non-strange light quark changes the  $S$ -wave hyperfine differences by at most a few MeV.

We next consider some measured  $P$ -wave heavy-light spin splittings. From [15] we find,

$$\begin{aligned} D_{s2} - D_{s1} &= 37.0 \pm 1.6 \text{ MeV}, \\ D_2^0 - D_1^0 &= 36.7 \pm 2.7 \text{ MeV}, \\ D_2^{\pm} - D_1^{\pm} &= 32 \pm 6 \text{ MeV}. \end{aligned} \quad (28)$$

Again we note the apparent vanishing of light quark mass dependence this time in a  $P$ -wave spin splitting. We conclude that spin splittings are only weakly dependent on the light quark mass. We will exploit this fact in section III C.

### B. The light quark mass dependence of a $1P-1S$ difference

In the preceding subsection we observed from experiment that both  $S$ -wave and  $P$ -wave heavy-light spin splittings (within a spin multiplet) were independent of the light quark mass. We next consider the mass splittings between pairs of states corresponding to different orbital angular momenta and examine the light quark mass dependence of this difference. We choose the  $D_1$   $P$ -wave state and the pseudoscalar  $D$  meson. The best measurements are

$$\Delta_u = D_1^0 - D^0 = 557.5 \pm 2 \text{ MeV}. \quad (29)$$

When the  $u$  light quark is replaced by a strange quark, the corresponding difference becomes

$$\Delta_s = D_{s1} - D_s = 567.3 \pm 0.4 \text{ MeV}. \quad (30)$$

The differences  $\Delta_u$  and  $\Delta_s$  are amazingly similar. We see that they differ by

$$\Delta = \Delta_s - \Delta_u = 9.8 \pm 2 \text{ MeV}. \quad (31)$$

### C. Conclusion for the spin-averaged $1P-1S$ difference

We demonstrated in Sec. III A that both  $S$ - and  $P$ -wave spin splittings are, within error and isospin uncertainty, independent of light quark mass. We may therefore conclude that the  $m$ -dependence of the difference  $\Delta_s - \Delta_u$  also represents the  $m$ -dependence of the spin-averaged  $1P-1S$  excitation energies. To show this explicitly, we write the HL meson mass as the sum of the heavy quark mass and the excitation energy,

$$M = m_Q + E. \quad (32)$$

We then separate the excitation energy into spin-averaged and spin-dependent parts,

$$E = E^{SA} + E^{SD}. \quad (33)$$

As in Eqs. (29) and (30), we define  $\Delta_s$  and  $\Delta_u$  to be the differences between  $P$ -wave ( $J^P = 1^+$ ) and  $S$ -wave ( $J^P = 0^-$ ) states, for strange and non-strange light quarks respectively. Using our observation that the spin-dependent parts are essentially independent of light quark mass, we see that the spin dependent parts will cancel in the difference  $\Delta = \Delta_s - \Delta_u$ . Thus

$$\Delta = (E_{1P} - E_{1S})_s - (E_{1P} - E_{1S})_u \quad (34)$$

measures the light quark mass dependence of the spin-independent  $1P-1S$  level difference.

Two main results emerge from this subsection. First, the light quark mass dependence is only about 2% of the measured level difference. This is a useful tool in the analysis of heavy-light spectroscopy [16]. Second, although it is small,  $\Delta$  is definitely not zero. We will use the actual value (31) to test the predictions of various assumptions about the nature of quark confinement.

## IV. COMPARISON WITH EXPERIMENT

We are now prepared to compare carefully the different confinement predictions with experiment. As we originally noted [16], the  $m$  dependences of all the heavy-light states are amazingly similar. We have also noted in Sec. II C that this universal  $m$  dependence is nearly satisfied in an analytical calculation. In the example with scalar confinement, the  $m$  slope for the difference  $1P-1S$  is about 30 times smaller than each separate slope. Furthermore, we noted in Sec. III B that when one compares two heavy-light states, one  $P$ -wave and one  $S$ -wave, the difference changes by less than 2% when a non-strange

light quark is replaced by a strange one. This change is not zero however, but for the  $D_1$  and  $D$  states has the experimental value (31)

$$\Delta = \Delta_s - \Delta_u = 9.8 \pm 2 \text{ MeV}. \quad (35)$$

In Fig. 1 we show the numerical mass splittings of heavy-light mesons for three different confinement scenarios, all with the same short range energy  $-k/r$ , and the same  $k = 0.5$ , as a function of light quark mass. Each of the three confinement scenarios has the same asymptotic confinement force,  $a = 0.18 \text{ GeV}^2$ . The upper curve assumes linear scalar confinement, the middle curve is the prediction of the relativistic flux tube and the lower curve linear time component vector confinement. In the scalar and time component vector potentials, the potentials  $S(r)$  and the long-range part of  $V(r)$  respectively are  $ar$ . In the case relativistic flux tube model the string tension is  $a$ .

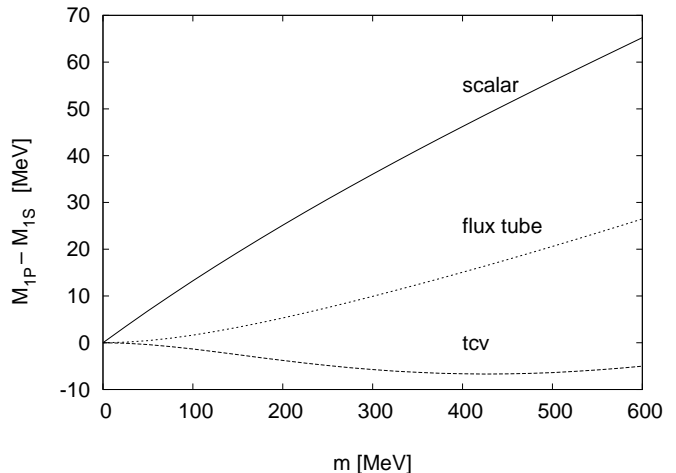


FIG. 1: Dependence of the  $1P-1S$  energy level difference on the light quark mass  $m$ . The numerical results compare different confinement mechanisms (all with the same long range confinement force  $a = 0.18 \text{ GeV}^2$  and all three calculations assume the same short range Coulombic constant  $k = 0.5$ .)

We note that the scalar confinement has the most rapid increase of the  $1P-1S$  difference as the light quark mass increases. The flux tube confinement is intermediate and time component vector linear confinement actually decreases slightly. Using the reasonable values for the strange quark mass (500 MeV) and the non-strange mass (300 MeV) [16], we find the following values for  $\Delta$ ,

$$\Delta_{\text{scalar}} = 19 \text{ MeV}, \quad (36)$$

$$\Delta_{\text{flux tube}} = 10 \text{ MeV}, \quad (37)$$

$$\Delta_{\text{TCV}} = -1 \text{ MeV}. \quad (38)$$

In comparing these values to the experimental value given in Eq. (31),

$$\Delta_{\text{exp}} = 9.8 \pm 2 \text{ MeV}, \quad (39)$$

we observe that both scalar confinement and time component vector confinement are quite inconsistent with the experimental result. However, the flux tube confinement prediction is in agreement with the experimental result. These results are depicted in Fig. 2.

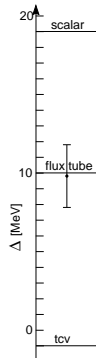


FIG. 2: The difference in the  $1P-1S$  energy gap between a light quark mass value of 500 MeV and 300 MeV. The experimental value is the dot below the 10 MeV level. All theoretical predictions have the same long range confinement force,  $a = 0.18 \text{ GeV}^2$ , and the same short range Coulombic constant,  $k = 0.5$ .

## V. DISCUSSION

### A. $m$ slopes and the $k$ value

The reader may have noticed that the  $m$  slope for the  $1P-1S$  difference calculated analytically (23) is about 0.02 whereas the  $m$  slope in Fig. 1 is about five times larger. This is because the Coulomb constant  $k$  is zero in the analytical result and has the more realistic value 0.5 in the numerical calculations shown in Fig. 1. The effect is magnified due to the strong cancelation in the  $1P-1S$  difference.

The choice  $k = 0.5$  is quite reasonable. As we noted in [16], the spin-averaged experimental value for  $E_{1P} - E_{1S}$  can be extracted from the  $D_s$  mesons;

$$E_{1P} - E_{1S} = 439 \text{ MeV}. \quad (40)$$

The appropriate choice of  $k$  is determined by computing the above quantity as a function of  $k$  as shown in Fig. 3. We conclude that the common value of  $k = 0.5$  assumed in the considerations of the last section was appropriate and that the effect of a slightly larger  $k$  would only make our conclusions stronger.

### B. Constituent quark masses

Another interesting result of a choice of confinement scenario is a constraint that relates the non-strange and

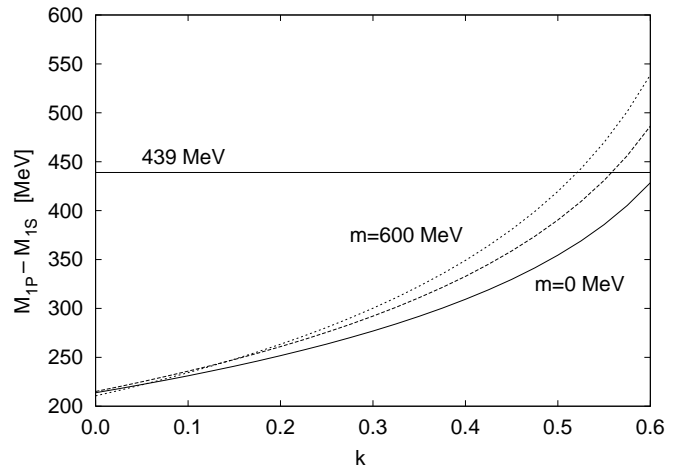


FIG. 3: The  $1P-1S$  level difference as a function of the Coulomb constant  $k$  for scalar confinement. In this case there is a noticeable dependence on the light quark mass  $m$  and we show the calculation for  $m = 0, 300$ , and  $600$  MeV. Since the experimental value was found for  $D_s$  mesons we see a value of  $k = 0.53$  is indicated with  $m = 500$  MeV.

strange light quark masses. This relation is the result of the measured value for the  $B_s$  and  $B$  mass difference,

$$B_s - B \simeq 91 \text{ MeV}. \quad (41)$$

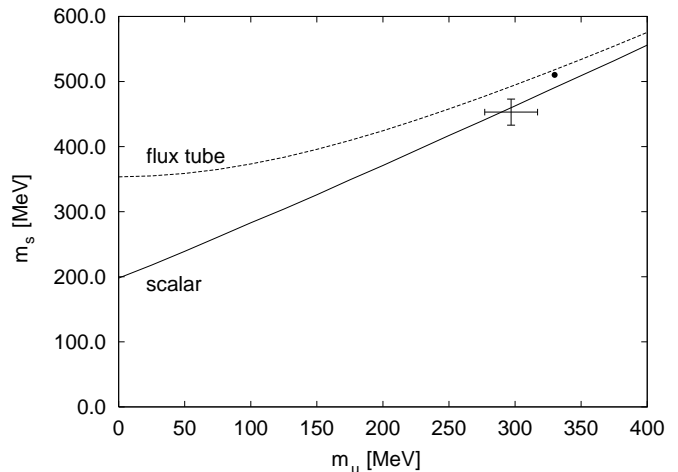


FIG. 4: The constraint between  $m_s$  and  $m_u$  light quark masses due to the measured  $B_s - B$  mass difference (41). The solid curve assumes scalar confinement while the dashed curve is due to flux-tube confinement. The “data” points are quark masses analyses of hyperon magnetic moments in the constituent quark model [15, 17].

In Fig. 4 we show this constraint scalar confinement and flux tube confinement scenarios. Although the curves differ considerably for small light quark mass, they are quite similar in the larger range. On the figure we show constituent quark masses obtained by analyses of hyperon magnetic moments [15, 17]. The result justifies

our choice of 500 MeV for the strange quark and 300 MeV for the non-strange quark.

## VI. CONCLUSIONS

Our points in this paper may be quickly summarized.

- From the data, we conclude that spin splittings do not vary with light quark mass value. We then can extract the change (31) in the spin-averaged  $1P-1S$  level difference as one replaces the non-strange by a strange light quark.
- We compare the predictions of the scalar potential, time component vector potential and flux-tube quark confinement scenarios with experimental results, as shown in Fig. 2. The conclusion is that flux-tube confinement works well while both scalar and time component vector confinement fail badly.

We observe therefore that scalar confinement has at least one specific point of disagreement with experiment. This complements the theoretical disagreements with QCD mentioned in the introduction.

### Acknowledgment

This work was supported in part by the U.S. Department of Energy under Contract No. DE-FG02-95ER40896.

## APPENDIX A: EXPECTATION VALUES

The principal aim here is to compute the expectation value of  $r^p$  with the harmonic oscillator wavefunctions (13),

$$\langle r^p \rangle = N_{n,\ell}^2 \int_0^\infty dr r^{2\ell+2+p} e^{-ar^2} \left[ L_{n-1}^{\ell+\frac{1}{2}}(ar^2) \right]^2. \quad (\text{A1})$$

A change of integration variable to the dimensionless combination  $z = ar^2$  yields

$$2a^{\ell+\frac{3}{2}+\frac{p}{2}} \langle r^p \rangle = N_{n,\ell}^2 \int_0^\infty dz z^{\ell+\frac{1}{2}+\frac{p}{2}} e^{-z} \left[ L_{n-1}^{\ell+\frac{1}{2}}(z) \right]^2. \quad (\text{A2})$$

It is helpful to use the Chu-Vandermonde sum formula [18],

$$L_{n-1}^\alpha(z) = \sum_{j=1}^n \frac{(\alpha-\beta)_{n-j}}{(n-j)!} L_{j-1}^\beta(z), \quad (\text{A3})$$

where the Pochhammer symbol  $(z)_N$  is defined as,

$$(z)_N = z(z+1)\cdots(z+N-1) = \frac{\Gamma(z+N)}{\Gamma(z)}, \quad (\text{A4})$$

$$(z)_0 = 1. \quad (\text{A5})$$

With the choices

$$\alpha = \ell + \frac{1}{2}, \quad (\text{A6})$$

$$\beta = \ell + \frac{1}{2} + \frac{p}{2}, \quad (\text{A7})$$

$$\alpha - \beta = -\frac{p}{2}, \quad (\text{A8})$$

we substitute Eq. (A3) into (A2) and use the orthonormality relation for Laguerre polynomials [18]

$$\int_0^\infty dz z^\beta e^{-z} L_j^\beta(z) L_{j'}^\beta(z) = \frac{\Gamma(j+\beta+1)}{j!} \delta_{jj'}, \quad (\text{A9})$$

to obtain our general result,

$$\langle r^p \rangle = a^{-\frac{p}{2}} \sum_{j=1}^n \left[ \left( -\frac{p}{2} \right)_{n-j} \right]^2 \binom{n-1}{j-1} \frac{\Gamma(j+\ell+\frac{1}{2}+\frac{p}{2})}{\Gamma(n+\ell+\frac{1}{2})(n-j)!}. \quad (\text{A10})$$

In Eq. (A10) we use the notation for the binomial coefficients,

$$\binom{n}{m} = \frac{n!}{m!(n-m)!}. \quad (\text{A11})$$

The specific result that is required in Sec. IIB is for the ground state ( $n=1$ ) is

$$\langle r^p \rangle_{n=1} = a^{-\frac{p}{2}} \frac{\Gamma(\ell+\frac{3}{2}+\frac{p}{2})}{\Gamma(\ell+\frac{3}{2})} \quad (\text{A12})$$

Some cases of direct interest are

$$p = -1 : \quad \langle r^{-1} \rangle = \sqrt{a} \frac{\Gamma(\ell+1)}{\Gamma(\ell+\frac{3}{2})}, \quad (\text{A13})$$

$$p = 0 : \quad \langle 1 \rangle = 1, \quad (\text{A14})$$

$$p = 1 : \quad \langle r \rangle = \frac{1}{\sqrt{a}} \frac{\Gamma(\ell+2)}{\Gamma(\ell+\frac{3}{2})}, \quad (\text{A15})$$

$$p = 2 : \quad \langle r^2 \rangle = \frac{1}{a} \left( \ell + \frac{3}{2} \right). \quad (\text{A16})$$

- 
- [1] E. Eichten, K. Gottfried, T. Kinoshita, J. Kogut, K.D. Lane, and T.-M. Yan, Phys. Rev. Lett. **34**, 369 (1975).
- [2] *Quarkonia* (W. Buchmüller, ed.) Current Physics-Sources and Comments Vol. 9, (North-Holland, 1992).
- [3] A.B. Henriques, B.H. Kellet, and R.G. Moorhouse, Phys. Lett. **64B**, 85 (1976).
- [4] N. Isgur, Phys. Rev. D **57**, 4041 (1998).
- [5] N. Brambilla and G. M. Prosperi, Phys. Lett. **236B**, 69 (1990); Phys. Rev. D **46**, 1096 (1992);
- [6] E. Eichten and F. Feinberg, Phys. Rev. D **23**, 2724 (1981).
- [7] D. Gromes, Z. Phys. C **26**, 401 (1984).
- [8] G. Bali, Phys. Rept. **343**, 1 (2001).
- [9] W. Buchmüller, Phys. Lett. **112B**, 479 (1982).
- [10] M.G. Olsson, C. Olson, and Ken Williams, Phys. Rev. D **45**, 4307 (1992).
- [11] T.J. Allen, M.G. Olsson, and J.R. Schmidt, Phys. Rev. D **69**, 054013 (2004).
- [12] Steve Jacobs, M.G. Olsson, and Casimir Suchyta III, Phys. Rev. D **33**, 3338 (1986); M.G. Olsson, S. Veseli and K. Williams, Phys. Rev. D **51**, 5079 (1995).
- [13] H. Hellmann, *Einführung in die Quantenchemie* (Deuticke Verlag, Leipzig, 1937); R.P. Feynman, Phys. Rev. **56**, 340 (1939).
- [14] L.P. Fulcher, Phys. Rev. D **50**, 447 (1994); C. Semay and B. Silvestre-Brac, Phys. Rev. D **52**, 6553 (1995); W. Lucha, F.F. Schöberl, Int. J. Mod. Phys. A **15** 3221 (2000); Phys. Rev. A **60**, 5091 (1999).
- [15] K. Hagiwara *et al.*, Phys. Rev. D **66**, 010001 (2002) and 2003 off-year partial update for the 2004 edition available on the PDG WWW pages (URL: <http://pdg.lbl.gov/>)
- [16] T.J. Allen, Todd Coleman, M.G. Olsson, and Siniša Veseli, Phys. Rev. D **69**, 074010 (2004).
- [17] Jerrold Franklin, Phys. Rev. D **66** 033010 (2002).
- [18] I.S. Gradshteyn and I.M. Ryzhik, *Table of Integrals, Series, and Products* (Academic Press, New York, 1980).